365 nm photon-induced dynamics of ClNO adsorbed on MgO(100)

H. Ferkel, L. Hodgson, J. T. Singleton, P. M. Blass, H. Reisler, and C. Wittig
Department of Chemistry, University of Southern California, Los Angeles, California 90089-0482

(Received 14 January 1994; accepted 3 March 1994)

Temperature programmed desorption (TPD) and 365 nm photolysis of ClNO adsorbed on MgO(100) at 90 K were investigated under ultrahigh vacuum conditions. The crystal was treated in a way that largely eliminated oxygen vacancies and yielded a relatively smooth surface. Angularly resolved time-of-flight (TOF) mass spectra and state-selective resonance-enhanced multiphoton ionization (REMPI) spectra of NO photoproducts were obtained. The TPD data indicate that ClNO desorbs at surface temperatures above 160 K for exposures (Θ) below 0.2 Langmuirs (L), while for higher values of Θ the main desorption peak is near 120 K. The higher temperature feature, which saturates at $\Theta\sim0.3$ L, is probably associated with binding to defect sites. Thermal desorption is believed to be molecular at all coverages. Irradiation at 365 nm for $0.1\leqslant\Theta\leqslant5.0$ L yields products having low average translational energies and broad translational energy distributions. NO fragment REMPI spectra were recorded at $\Theta\geqslant0.7$ L. The rotational distributions could be fit with a temperature of 110 ± 10 K, i.e., comparable to that of the substrate. These results differ from those obtained in the photodissociation of gas-phase ClNO, where the NO fragment has high translational and rotational energies. However, the present results are similar to those obtained on rougher MgO(100) surfaces. Possible mechanisms are discussed.

I. INTRODUCTION

Experimental and theoretical studies of the photochemistry and photophysics of molecules adsorbed on dielectric crystals constitute a rapidly growing field.[1–31] The transparency of such materials in the visible and near ultraviolet facilitates direct excitation of the adsorbate and may lead to dissociation on a shorter time scale than that required for energy transfer to the crystal. Thus, the photochemistry and photophysics of species adsorbed on insulators may differ markedly from the corresponding processes on metal surfaces. Direct adsorbate photolysis has been observed on LiF,[1–3,6–8,10,11,14,15,18–22,29] Al_2O_3,[4,5,9,12,13,23,25] and MgO,[24,28,30,31] and has been treated theoretically for the cases of LiF[26,27] and MgO.[16,17,30] Initially, it was thought that insulators cause only minor perturbations to the electronic structure of the adsorbate, the main effect being to orient the adsorbate on the surface. This was the case, for example, in the photodissociation of methyl iodide on MgO(100). However, the emerging picture is that in certain cases the insulator can have a profound effect on the photophysics and photochemistry, and surface preparation can affect results as well. For example, in the 222 nm photodissociation of CH_3Br on LiF(100), the CH_3 fragment departing from a rough LiF(100) surface has much less translational energy than the same fragment departing from an annealed LiF(100) crystal,[2] or generated in the corresponding gas-phase photodissociation.[32]

Recently,[31] we showed that the 365 nm photolysis of ClNO adsorbed on rough MgO(100) at $\Theta>0.5$ L yields fragments with very low internal and translational energies relative to gas-phase ClNO photodissociation.[33–35] It was postulated that ClNO grows on MgO(100) in islands with defects serving as nucleation centers, and that photofragment rotational and translational energies are quenched by collisions with other molecules in the island or with the surface. The large differences observed between the gas-phase and surface behavior in ClNO photolysis can be contrasted with the smaller differences observed in some other systems involving smoother surfaces.[35] The latter include the 257 nm photodissociation of methyl iodide on MgO(100)[24,28,30] and the 248 nm photolysis of NO_2 on annealed LiF(100).[29] It is thus important to establish how ClNO behaves on smoother MgO(100) crystals and also at lower coverages, where collisions of the fragments with other adsorbed molecules may be less likely.

In the work reported here, thermal desorption as well as 365 nm photoexcitation of ClNO adsorbed at 90 K on MgO(100) surfaces, in which oxygen vacancies were largely eliminated by annealing in O_2, are examined for exposures $\Theta>0.1$ L. Photolysis is examined for different polarizations and angles of incidence between the photolysis laser beam and the surface, and different photofragment ejection angles are probed. All experiments are carried out with much smoother surfaces than were used previously.[31] Species emanating from the surface are detected by using a quadrupole mass spectrometer (QMS) to obtain time-of-flight (TOF) distributions, while NO state distributions are determined by resonance-enhanced, two-photon, two-frequency ionization (REMPI). At 365 nm, gaseous ClNO is excited via a parallel transition, $S_3(2\,^1A')\leftarrow S_0(1\,^1A')$, yielding rotationally hot NO (i.e., $J''_{peak}=46.5$)[34] almost exclusively in $v''=0$.

With rough surfaces and exposures above 0.5 L (but using the same diagnostic techniques),[31] we found that the TOF distributions were considerably slower than for the corresponding gas-phase photodissociation process.[33] There was no evidence for rapid ejection of products from the surface. Likewise, NO rotational distributions were cold and could be fit with $T_{rot}=100-140$ K, which differed greatly from the highly nonstatistical gas-phase distributions. These results, together with temperature programmed desorption (TPD) data, suggest that ClNO photolysis is dominated by strong

 0021-9606/94/100(12)/9228/10/$6.00

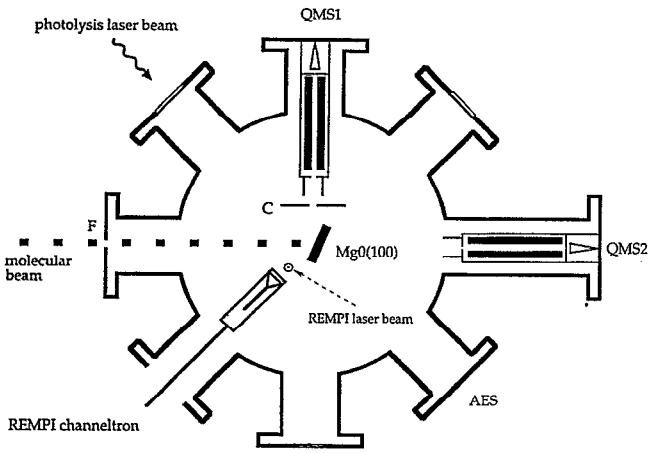

FIG. 1. Schematic of the UHV chamber used for the TPD and photoexcitation experiments. The buffer and molecular beam source chambers are not shown. The rotatable crystal is located at the center of the main chamber. Desorbed and/or photon-induced products are detected with a quadrupole mass spectrometer, QMS1, oriented perpendicular to the molecular beam. The photolysis light enters the chamber at 45° relative to the molecular beam and QMS1. The probe laser enters from below. The distance between the surface and the QMS1 ionizer is 8.5 cm.

attractive interactions with its surroundings and that ClNO aggregates on the surface as islands, nucleating around defect sites.

The behavior observed with smoother surfaces (including exposures below 0.5 L) is similar to that observed with rough surfaces. We conclude therefore that interactions with the environment (i.e., other adsorbate molecules and/or the surface) are mainly responsible for the loss of energy for rough and smooth surfaces alike. TPD experiments highlight the role of defect sites, e.g., in inducing increased binding. The possibility that electronic interactions at defect sites or between the surface and the electronically excited ClNO may alter the photodissociation dynamics as discussed as well. The roles of direct photodissociation of the adsorbate and of desorption of intact ClNO in the photon-induced process are examined.

II. EXPERIMENT

The experimental arrangement has been described elsewhere.[36] Thus, only a brief description is given here, emphasizing modifications to the pumping system and the QMS arrangement. The machine consists of three vacuum chambers: a source chamber containing a pulsed nozzle, a buffer chamber, and an ultrahigh vacuum (UHV) chamber. The UHV and buffer chambers are pumped separately by turbomolecular pumps having speeds (for N_2 of 500 ℓ/s (Balzers TPU 520) and 230 ℓ/s (Balzers TPU 240), respectively. Both pumps are backed by a single diffusion pump. The UHV chamber can be evacuated to 1×10^{-10} Torr.

The UHV chamber (Fig. 1) is equipped with an Auger electron spectrometer (AES), two quadrupole mass spectrometers (QMS1 and QMS2), an Ar atom sputter gun (not shown), a bare channeltron for REMPI detection, and a resistively heated Mo sample holder that is electrically insulated from a rotatable liquid nitrogen reservoir by a sapphire disk. Surface temperatures could be varied from 90 to 1050 K. Temperatures were measured with a chromel–alumel thermocouple attached to the Mo block to which the MgO was clamped. In some experiments, a 3×4 mm^2 hole in the sample holder enabled the photolysis beam to pass through the sample without hitting the holder.

A pulsed nozzle driven by a piezoelectric crystal (Physik Instrumente) was used in the He diffraction measurements and to dose ClNO onto the crystal. In the latter, neat ClNO at 40 Torr backing pressure was used; coverage was directly proportional to dosing exposure.[31] The ClNO (Matheson, 99.2%) was purified by several freeze-pump-thaw cycles with pentane slush.

The ClNO coverage was calibrated by using a molecular beam of nitrogen as a reference as follows. A gate valve between the source chamber (SC) and the buffer chamber (BC) could be operated in the open, blocked, or closed positions. In the blocked position the molecular beam still enters the buffer chamber but its direct path into the UHV chamber (UC) is blocked. Depending on these gate positions, different pressure increases in BC (Δp_{BC}) and UC (Δp_{UC}) were measured. In the blocked position, the flux j of N_2 molecules from BC to UC through an aperture F (1.2×4 mm^2, see Fig. 1) depends on Δp_{bc} and the mean velocity of N_2 molecules in BC. The number of molecules per unit time that travel from BC to UC is given by $m_{bl}=j\times F$. The flux into the buffer chamber was negligible, since $\Delta p_{\mathrm{BC}}\gg\Delta p_{\mathrm{UC}}$. ($\Delta p_{\mathrm{UC}}$ is also proportional to j). By opening the gate valve completely, a further pressure increase, $\Delta p'_{\mathrm{UC}}$, in UC was observed, while Δp_{BC} remained constant. $\Delta p''_{\mathrm{UC}}$ was attributed to those N_2 molecules in the beam, m_{beam}, that traveled directly through F. Since $m_{\mathrm{beam}}/(m_{bl}+m_{\mathrm{beam}}) = \Delta p_{\mathrm{UC}'}/(\Delta p_{\mathrm{UC}}+\Delta p_{\mathrm{UC}'})$, we obtain that $m_{\mathrm{beam}} = m_{bl}\Delta p_{\mathrm{UC}'}/\Delta p_{\mathrm{UC}}$ is the number of N_2 molecules that strike a small area (2.4×8 mm^2) of the MgO(100) surface after passing through F. The ClNO beam was then generated under identical pulsed-nozzle conditions, and therefore the ratio of N_2 and ClNO molecules passing through the nozzle was equal to the ratio of their mean beam velocities. An absolute calibration of the ClNO dosage was achieved by determination of the pressure increase, Δp_{SC}, in SC for N_2 and ClNO under the same source conditions. In this paper, the dosage is given in units of Langmuirs (1 L$=10^{-6}$ Torr s).

In the TPD measurements, ClNO was detected with QMS1. A 12×8 cm^2 plate was installed between QMS1 and the crystal to minimize irradiation of the surface by photons and electrons emanating from the QMS1 filament. The shield had four vertically arranged apertures of different diameters (1–4 mm) that could be moved externally into position in front of the surface. Positioning one of these apertures between QMS1 and the crystal enabled only particles emitted from a correspondingly limited area of the crystal surface to reach QMS1 by a direct path.

Single crystal MgO (Marketech International) was cleaved in air and mounted immediately on the sample holder; within 5 min the UHV chamber was evacuated to $<10^{-7}$ Torr. The substrate and chamber were then baked at ~400 K for 15 h and the crystal was subsequently annealed for 3 h in 10^{-5} Torr of O_2 at 1000 K to remove oxygen

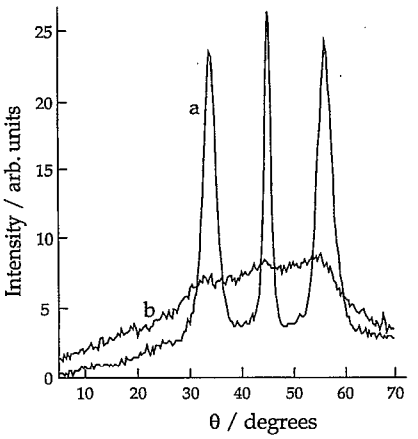

FIG. 2. Scattered He intensity as a function of angle between the He atom beam and the MgO(100) surface normal. Curve (a) was obtained after annealing the cleaved crystal in 1×10^{-5} Torr of O_2 for 3 h at 1000 K. Curve (b) was obtained with a polished crystal annealed without oxygen at 700 K (Ref. 31). The incident He wave vector was ~3 Å^{-1}, and the angular resolution was ~5%. The crystal was maintained at 90 K.

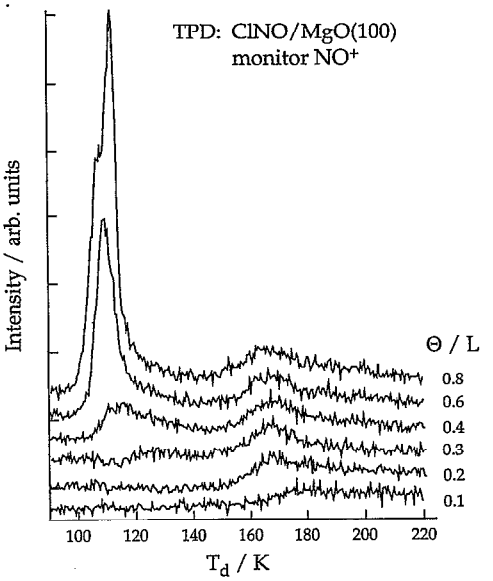

FIG. 3. TPD spectra of ClNO on MgO(100) at exposures Θ=0.1–0.8 L. Displayed are the NO^+ intensities obtained as a function of desorption temperature following various exposures. The ClNO molecule completely fragmented the QMS1 ionizer.

vacancies. It has been shown by electron energy loss spectroscopy (EELS) experiments that oxygen vacancies can be largely removed by annealing the crystal.[37] After this treatment AES traces showed no surface impurities, as in Ref. 38, and He scattering revealed a sharp diffraction pattern, as shown in Fig. 2, curve (a).

Two other commercial MgO crystals were also used: Goodfellow Corporation and Atomergic Chemetals Corporation; both were cleaved in air by the manufacturers. One of these, polished by the manufacturer after cleaving, was used in Ref. 31. Figure 2, curve (b) displays its He scattering curve, indicating no diffraction peaks. He diffraction is a sensitive and nondestructive tool for investigating surface properties of MgO and other insulators.[39] Annealing in O_2 also removed residual surface carbon, which was still present after annealing for 6 h without O_2. Fast argon bombardment removed carbon, but after annealing (for 10 h, either with or without O_2) a less sharp He diffraction pattern was observed. In summary, the best surface quality was achieved with a crystal that was cleaved in our laboratory and immediately evacuated and annealed in O_2. This crystal had a much less disturbed surface than the rough crystal used previously,[31] presumably due to the removal of oxygen vacancies. However, steps and kinks on the surface are more difficult to estimate and control, e.g., a cleaved MgO(100) surface was estimated to have one step per μm.[39(c)]

The 365 nm photolysis radiation was from an excimer-laser-pumped dye laser (Questek 2200 and Lambda Physik Fl 2002). The beam was expanded and collimated to 3.5 mm diam before entering the UHV chamber, providing a fluence of ~650 μJ/cm^{-2}. A photoelastic modulator (PEM) provided polarization rotation of the photolysis radiation without requiring realignment of the photolysis beam. The probe system was described elsewhere.[36] The 226 and 280 nm beams entered the UHV chamber from below, with NO ionization occurring 2–3 cm from the surface via excitation of the $\gamma(0-0)$ transition near 226 nm (~4 μJ) followed by 280 nm photoionization (~1 mJ).

Since adsorbed NO and ClNO have different TPD features (see Sec. III), contributions to the TPD signals from NO contamination (e.g., in the ClNO samples) could be checked. Such contamination was checked by TPD before and after each ClNO experiment. The data reported here are free from NO contamination.

III. RESULTS

The results of the TPD measurements are shown in Figs. 3 and 4. The intensities of the NO^+ signals monitored by QMS1 for different ClNO exposures are displayed as a function of surface temperature for a constant heating rate of 0.5 K s^{-1}.[31] The parent $ClNO^+$ ion was not observed in the mass spectrometer due to efficient fragmentation in the ionizer. The Cl^+ signal (not shown) shows the same TPD behavior, indicating that ClNO desorbs molecularly from the surface at both low and high coverages. For $\Theta<0.2$ L, ClNO desorbs at $T_d>160$ K. With increasing Θ, the maximum at $T_d\sim165$ K saturates in intensity and a second peak appears at lower T_d. This peak, which appears at ~125 K at Θ=0.3 L, is shifted by ~15 K to lower temperatures as the exposure is increased to 0.6 L. Figure 4 shows that at 0.8 L a narrow peak is superimposed on the broad maximum, which is the only feature at 0.6 L, and at higher coverages desorption follows zeroth-order kinetics. All signal intensities depend linearly on the area of the collimator hole inserted between QMS1 and the crystal (see Sec. II).

The TOF measurements were carried out by monitoring either NO^+ or Cl^+ with QMS1 as a function of arrival time after the photolysis pulse. Typically 30 laser shots at a 10 Hz repetition rate were used per spectrum. The geometric ar-

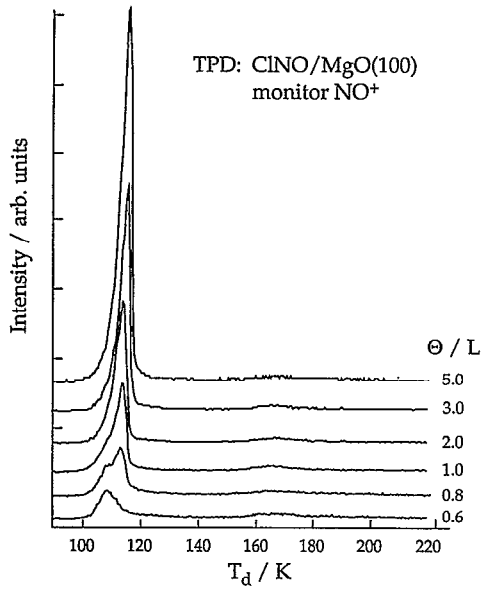

FIG. 4. TPD spectra of ClNO on MgO(100) at exposures Θ=0.6–5.0 L. Displayed are the NO^+ intensities obtained as a function of desorption temperature following various exposures. The ClNO molecule completely fragmented in the QMS1 ionizer.

rangements are shown in Fig. 5. In the raw TOF data obtained by monitoring NO^+, a longer tail was observed than in traces obtained by monitoring Cl^+, as shown in Fig. 6, curve (a). This could be attributed to background NO; Cl does not have a background contribution, since it is removed by collisions with the chamber walls. The TOF data could be corrected for this background contribution by positioning a collimator between QMS1 and the crystal in two different locations (Fig. 1), while monitoring the NO signal. In one measurement, a 3-mm-diam collimator was positioned between QMS1 and the crystal, thereby allowing some of the desorbed particles to follow a direct path to QMS1; see Fig. 6, curve (a). Alternatively, when the direct path from the surface to QMS1 was blocked, only background was observed, as shown in Fig. 6, curve (b). Curve (c) shows the difference between the traces, which is the *corrected* TOF distribution. All TOF spectra presented below were obtained in this manner and were also corrected for the velocity dependence of the ionization efficiency and for the ion flight time in QMS1.

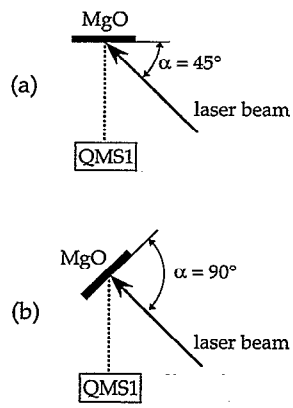

FIG. 5. Schematic of the experimental arrangement used in the TOF measurements. α is the angle between the photolysis beam and the MgO(100) surface.

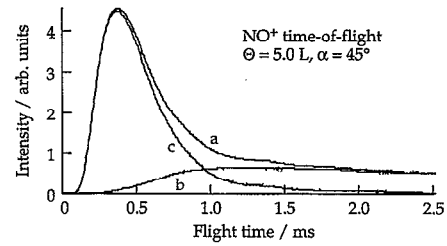

FIG. 6. NO^+TOF signals monitored with QMS1 after 365 nm photolysis of 5.0 L of ClNO adsorbed on MgO(100). The experimental arrangement is shown in Fig. 5(a). Curve (a) shows the raw data, curve (b) shows the background NO signal, and curve (c) is the corrected TOF curve (see the text for details). The velocity dependent detection efficiency and the ion flight time in the QMS have not been taken into account.

The TOF traces obtained by monitoring NO^+ and Cl^+ at different ClNO coverages are shown in Figs. 7 and 8. In these experiments, two configurations were used that differed both in the photolysis beam of incidence (α) and the detection angle (Fig. 5). The TOF distributions were much colder and broader, even at low coverages, than those resulting from the photodissociation of ClNO in the gas phase,[33] and were similar to those obtained with the rough ClNO surface.[31] The average translational energy following surface photolysis was ~10 meV, with a Boltzmann-type distribution at $T \approx 100$ K, while in the gas-phase photodissociation, the Cl

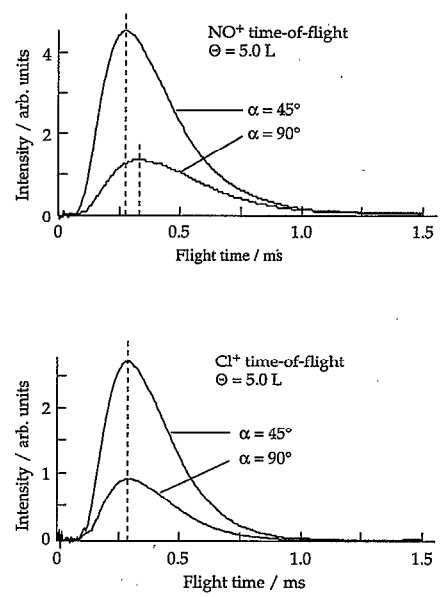

FIG. 7. NO^+ and Cl^+ TOF spectra monitored with QMS1 after 365 nm photolysis of ClNO adsorbed on MgO(100). The spectra were obtained at α=45° and 90° (see Fig. 5) following exposure of 5.0 L of ClNO. The velocity dependent detection efficiency and the ion flight time in the QMS have been taken into account.

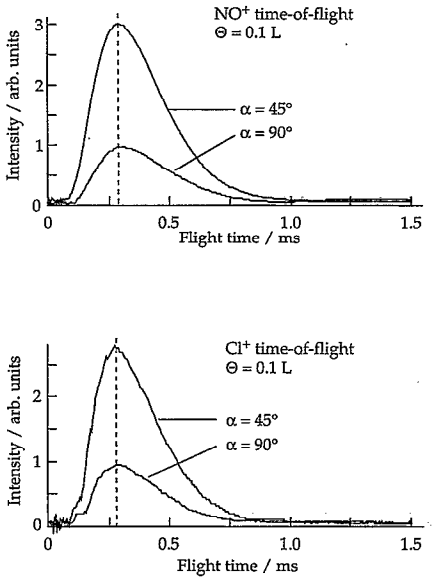

FIG. 8. NO^+ and Cl^+ TOF spectra monitored with QMS1 after 365 nm photolysis of ClNO adsorbed on MgO(100). The spectra were obtained at α=45° and 90° (Fig. 5) following exposure of 0.1 L of ClNO. The velocity dependent detection efficiency and the ion flight time in the QMS have been taken into account.

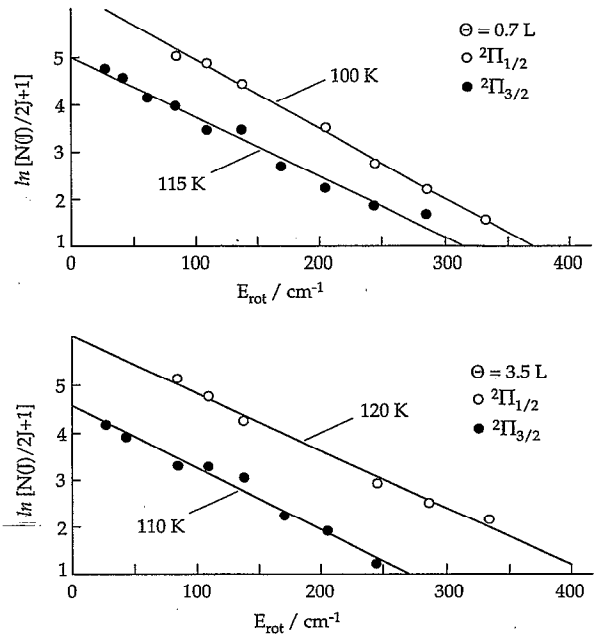

FIG. 10. NO v''=0 Boltzmann plots for the $^2\Pi_{1/2}(R_{11}+Q_{21})$ and $^2\Pi_{3/2}(Q_{22}+R_{12})$ spin–orbit states, obtained following 365 nm photodissociation of ClNO adsorbed on Mg(100) at two different ClNO exposures. The distributions are well represented by a temperature of 110±10 K.

and NO fragments had 580 and 670 meV of translational energy, respectively. This is surprising *if* one assumes only a modest interaction between the surface and the adsorbate and notes the transparency of MgO at 365 nm.

In the range $0.1 \leqslant \Theta \leqslant 5$ L, the Cl^+ TOF distributions were independent of Θ and the experimental crystal-laser-QMS geometry (Fig. 5). In the case of NO^+, the peaks in the TOF traces observed at high Θ and α=90° were shifted to slightly lower kinetic energies relative to the traces obtained at α=45°. As can be seen in Fig. 9, this shift in the peak location first occurred in Θ=0.3 L, which coincided with the saturation in the intensity of the broad 165 K peak in the TPD spectrum (Fig. 3).

TOF measurements were also carried out with different polarizations of the photolysis radiation. Specifically, its electric field **E** was oriented either in the plane defined by the incident laser beam and the line between the surface and QMS1 (*p* polarization) or perpendicular to this plane (*s* polarization). For the arrangement shown in Fig. 5(b), the spectra (including intensities) were not expected to change, since **E** lies parallel to the substrate for both polarizations. This was confirmed experimentally. The situation was different for the case shown in Fig. 5(a). With *p* polarization, only the projection of **E** on the surface could excite molecules in the same way as at α=90°, assuming direct excitation of the adsorbate and flat-lying ClNO. Therefore, a change in the intensity of the TOF spectra monitored for *s* and *p* polarization may be anticipated if ClNO is preferentially oriented parallel to the surface. However, no such dependence was observed. This is consistent with no globally preferred orientation of ClNO on the surface.

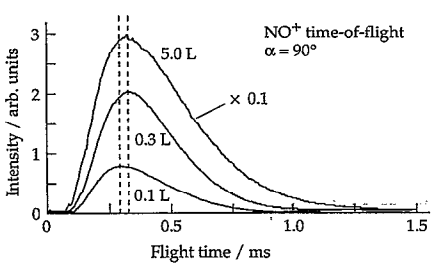

FIG. 9. NO^+ time-of-flight spectra monitored with QMS1 after 365 nm photolysis of ClNO adsorbed on MgO(100). The spectra were obtained at α=90° (Fig. 5) following various exposures. The velocity dependent detection efficiency and the ion flight time in the QMS have been taken into account.

NO product was detected directly by using REMPI.[31] The spectra were measured under conditions where steady-state surface coverage of the molecules was maintined for Θ values of 0.7–3.5 L, as described before,[31] and the NO detection angle and photolysis laser power were kept constant throughout the measurement. The rotational distributions of the NO products were determined from the spectra as described before,[31] and are well represented by a Boltzmann distribution at T_{rot}=110±10 K, independent of coverage and other experimental conditions. Two representative Boltzmann plots are shown in Fig. 10. The distributions are very different from the results obtained in gas phase photodissociation experiments,[34] but are similar to those obtained with the rough surface.[31] Figure 11 compares the NO rotational populations obtained in the photodissociation of ClNO adsorbed on MgO(100) and in the gas phase.

The NO TOF distributions at $\Theta \geqslant 0.7$ L were also mea-

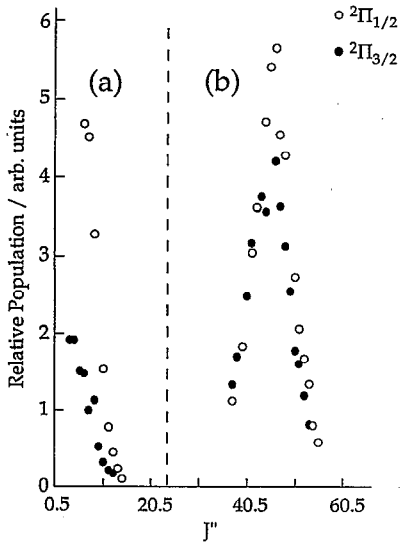

FIG. 11. NO $v''=0$ rotational distributions obtained following: (a) 365 nm photodissociation of 0.7 L of ClNO on MgO(100). The open and filled circles show distributions obtained by monitoring the $(R_{11}+Q_{12})$ and $(Q_{22}+R_{12})$ lines, respectively. (b) 355 nm gas-phase photodissociation of ClNO (from Ref. 34). The open and filled circles show distributions obtained by monitoring the Q_{11} and Q_{22} lines, respectively.

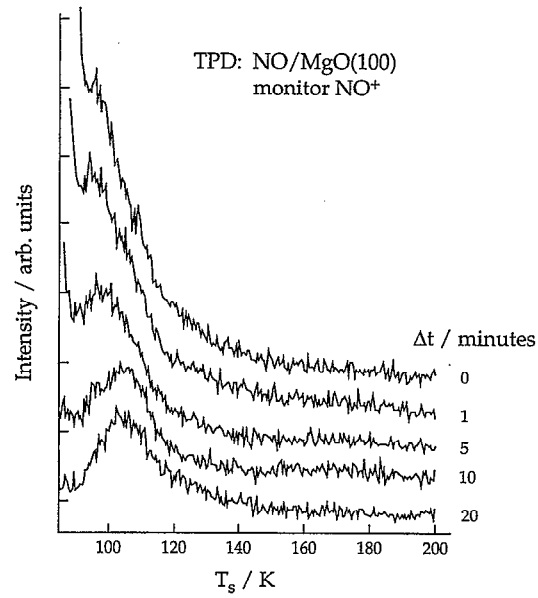

FIG. 12. TPD spectra of NO on MgO(100). Displayed are the NO^+ intensities in QMS1 as a function of desorption temperature for various time delays Δt between the dosing of ~3.0 L of ClNO and the start of the TPD measurements.

sured using REMPI detection by varying the time delay between the photolysis and probe lasers, and were found to be the same as those determined mass spectrometrically. The internal state distributions of NO in the fast and slow parts of the NO TOF distribution were similar.

In order to further understand the interactions of the photolytically formed NO fragments on the surface, and to investigate the possibility of dissociative adsorption of ClNO on MgO(100), separate TPD and laser-induced desorption (LID) experiments were carried out with pure NO. Although most of the dosed NO desorbed at $T_d<85$ K, the lowest attainable crystal temperature in our apparatus, a small amount of NO remained on the surface even at higher temperatures. This more strongly adsorbed NO was revealed by carrying out delayed TPD experiments after dosing. Figure 12 shows TPD data obtained after varying time delays, Δt, between dosing of ~3 L NO and the start of the TPD data acquisition. The traces demonstrate clearly that the major fraction of NO desorbs below 85 K. However, a small fraction remains on the surface and desorbs at $T_d\sim105$ K.

In a second experiment, the 90 K crystal was irradiated at 365 nm 20 min after dosing with NO and the TOF spectrum of the desorbed NO was measured (Fig. 13). The TOF spectrum was similar to those obtained in the photolysis of ClNO on MgO(100). A contribution to the TOF spectra in the ClNO/MgO(100) experiments from photodesorption of NO (originating, for example, from partial dissociative adsorption of ClNO or the readsorption of ClNO photofragments) therefore cannot be ruled out. The NO rotational distribution from the photodesorbed NO in the NO/MgO(100) LID experiment could not be extracted due to the large NO background caused by the small sticking coefficient of NO on MgO(100) at ~90 K.

TPD experiments carried out after irradiation of the adsorbed ClNO showed only a reduction in the amount of adsorbed ClNO; no new features were observed, and in particular, there was no evidence of a TPD signal at $T_d\sim85$ K, as was observed with direct NO exposure. Thus, though NO has a significant residence time on MgO(100) at 85 K (Fig. 12), there is no evidence that NO fragments from ClNO photolysis remain adsorbed. Likewise, no dissociation products were detected on the crystal at 300 K by AES either after TPD or photolysis. Furthermore, even after collisions of fast electrons (500 eV) with ClNO adsorbed on 90 K MgO(100) no dissociation fragments remained on the crystal. In this experiment, TPD spectra were taken after irradiating the ClNO covered surface with electrons from the AES electron gun for different periods of time. Again, no new TPD features were observed after irradiation—only a reduction in signal level.

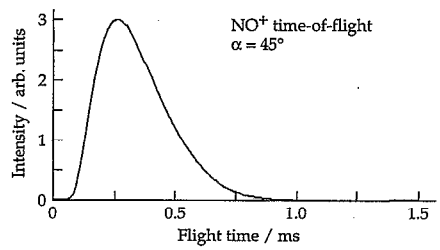

FIG. 13. TOF spectrum of NO^+ monitored with QMS1 after 365 nm photolysis of NO adsorbed on MgO(100). The spectrum was obtained at $\alpha=45°$ (Fig. 5), ~20 min after dosing 3.0 L of NO. The velocity dependent detection efficiency and the ion flight time in the QMS have been taken into account.

An important aspect of this study concerns the broad TOF distributions (compared to gas-phase photolysis) obtained using both mass spectrometric and REMPI detection which extends to >1 ms. One possibility that needed to be checked was that light absorption by the Mo sample holder did not induce desorption of species (ClNO or remaining photofragments), for example, by phonons traveling from the holder to the MgO(100) surface. To eliminate this effect, the sample holder with the rectangular hole was used (see Sec. II), and the photolysis laser was collimated to 1.0 mm diam to allow free passage through the hole. No difference in the TOF traces was observed when shining the light through the hole or in locations on the crystal that faced the sample holder.

IV. DISCUSSION

A. Temperature programmed desorption

The TPD of ClNO on MgO(100) shows two peaks: one at ~165 K that saturates at Θ=0.3 L and a second near 115 K that grows with Θ. An estimate using atomic van der Waals radii shows that ClNO lying flat on the surface covers and area of about 8 Å^2. For a sticking probability of unity and two dimensional (2D) growth, 0.3 L exposure covers the surface with less than 0.12 monolayers of adsorbed ClNO. A limited number of sites must be involved in the 165 K peak to explain its early saturation, and these probably involve defects. The higher desorption temperature indicates that binding to the defects is stronger than to the defect-free surface, as is usually the case. The broadness of the 165 K peak is consistent with a variety of defect sites and/or a variety of binding configurations at these sites.

The temperatures at which exposures were carried out prior to TPD were only ~25 K lower than the main TPD peak near 115 K. Thus, we assume that following adsorption ClNO molecules bound to the surface are labile and may collide with other "walkers"[40] as well as with islands and defects. The saturated peak at 165 K can be attributed to a limited number of defects binding a limited number of ClNO molecules.[31] At higher exposures, defect-free areas become covered, presumably beginning with sites adjacent to the decorated defects. In this picture, adlayer growth over defect-free areas is in the form of 2D islands, nucleated by defects and decorated defects.[31] It should be noted that islands formed randomly on a defect-free area are not necessarily stable and can decay before exceeding the critical size needed to become stable.[41] Therefore, the density on the surface during dosing can have an influence on the ultimate size distribution of islands, at least at low coverages.

Desorption between ~130 and 110 K is attributed to molecules evaporating from defect-free areas, perhaps at the edges of islands.[31] The desorption peak is seen to shift to lower temperatures with increasing exposure between 0.3 and 0.8 L (Fig. 3). In general, such a shift can be explained by a variety of phenomena including recombinative desorption following dissociative adsorption, collision-mediated desorption, and repulsive lateral interactions. Each is discussed briefly below.

Dissociative adsorption followed by recombinative desorption can be discounted as an explanation for the observed TPD shift. In this case, $Cl_{(a)}$ could react with other $Cl_{(a)}$ atoms or with $ClNO_{(a)}$ to form Cl_2.[42] The binding energy of Cl_2 to a perfect MgO(100) surface has been calculated to be 4.1 kcal mol^{-1} for a perpendicular binding geometry.[43] Thus, Cl_2 is likely to desorb as soon as it is formed; it certainly will have a very short residence time. Yet the mass spectrum following TPD of $ClNO_{(a)}$ is the same as that of gas-phase ClNO. Also, the data of Fig. 12 indicate that free $NO_{(a)}$ would be observable in TPD below 110 K. This is not observed. The evidence thus suggests that ClNO is adsorbed intact on MgO(100) with the possible exception of strongly binding defect sites.[31]

The possibility of repulsive lateral interactions between adsorbed ClNO molecules can be ruled out as well. At ~0.8 L, desorption starts to follow zeroth-order kinetics, an indicator of multilayer behavior at the desorption site. Referring again to the estimate based on van der Waals radii, we see that an exposure of 0.8 L cannot cover the surface. The appearance of zeroth-order kinetics does not imply completion of a monolayer, but suggests formation of three-dimensional (3D) islands. The data presented in Fig. 4 indicate that at exposures above 0.8 L the 3D islands are more stable with respect to thermal desorption than is the adlayer. These observations argue against an active role by repulsive lateral interactions, as do other indications of islanding discussed below. It is possible in some systems for lateral interactions to be attractive at low exposures and to become repulsive as the adlayer becomes more crowded. However, in the case of ClNO/MgO(100), crowding in the coverage regime where the TPD shift occurs is insignificant.

Though it is important to establish that ClNO/MgO(100) adsorption is not dissociative and that islanding occurs, a detailed understanding of the thermal desorption kinetics is not critical to the discussion of the observed photon-induced dynamics. We suggest, nevertheless, that the explanation of the observed TPD shift between 0.3 and 0.8 L may involve collision-mediated desorption. In such a mechanism, desorption occurs upon collision of one mobile adsorbate molecule with another, or with an island or cluster, and may involve formation of a precursor state prior to desorption. The order of the desorption is then >1, accounting for the observed shift.

TPD spectra of neat NO obtained at various delays between exposure and the start of data acquisition demonstrate attractions between NO and the surface of sufficient strength to cause adsorbed NO above 85 K with a residence time of minutes (Fig. 12). Therefore, we expect that TPD of NO at lower substrate temperatures would reveal a desorption peak below (but close to) 85 K. The length of the NO residence time at 85–90 K is significant to the interpretation of the laser photolysis experiments discussed below. NO formed with little translational energy, or having lost enough translational energy through collisions, may be trapped on the surface for significant periods of time.

Recall that a small amount of NO remains on the surface even 20 min after exposure and desorbs only near 105 K. Again, these results are consistent with a limited number of surface sites, probably defects, that allow NO to stick above

90 K. The amount of the strongly bound NO (found by integration of NO from 85 to 220 K) is similar to the amount of ClNO desorbing at $T_d \geq 160$ K in the ClNO/MgO(100) TPD experiments. Also of note is the fact that in the photon-induced experiments, the NO^+ signal intensities monitored by the mass spectrometer are similar at exposures where the higher temperature TPD peaks for ClNO (165 K) and NO (105 K) are just saturated.

B. Photon-induced dynamics

The main observations in these experiments are summarized here. For the ClNO/MgO (100) system, TOF spectra recorded with QMS1 for $m/e=35$ (Cl^+) and 30 (NO^+) indicate that the species released from the surface have low translational energies. As with rough surfaces,[31] no fast fragments are observed. The velocity distributions in the two channels are nearly the same, except for a slight shift in the peak of the NO^+ TOF traces at some exposures and detection angles. The velocity distributions measured at $m/e=35$ and 30 for ClNO/MgO(100) also closely match those observed via REMPI detection of NO. NO observed by REMPI after photolysis of ClNO/MgO(100) is rotationally cold, i.e., almost equilibrated with the surface. Variation of the photolysis laser polarization has no effect on the TOF signatures. Cl_2 is not observed. In the case of NO/MgO(100), TOF spectra of NO desorbed from MgO(100) reveal a translational energy distribution similar to that of fragments deriving from ClNO photoexcitation. Furthermore, signal intensities are comparable at low coverages for the two cases.

The similarity in the TOF traces obtained when monitoring Cl^+ and NO^+ in QMS1 raises the possibility only that intact ClNO (which fragments completely in the ionizer) leaves the surface. However, the REMPI data show conclusively that NO is produced as a photodissociation product. By varying the delay between the photolysis and probe lasers while holding the probe wavelength constant, we can generate TOF spectra for NO that have the same shapes and peak positions as those measured by the QMS. This NO is also rotationally cold, and has clearly equilibrated with the surface prior to desorption. It cannot derive from ClNO photodesorbed intact because the probe laser fluences are kept low enough to avoid dissociation by the probe followed by two-photon REMPI (three photons in all). Furthermore, if the three-photon process did occur, the resulting NO would have been rotationally hot. It is possible that QMS1 monitors both desorbed ClNO and photofragments, and that the photodesorbed ClNO has the same TOF spectrum as the Cl and NO photofragments (see below).

It is clear that significant cooling of photofragments occurs in these experiments. In the photolysis of gas-phase ClNO at 365 nm. 1.8 eV is available for fragment internal, and c.m. translational energies. However, the present TOF and REMPI results account for less than 0.1 eV. Below, we discuss several mechanisms that can result in such modest product excitations.

Bulk MgO is known to be permeated by defects,[44] the most common being oxygen vacancies, which introduce electronic states into the band gap[37] and could be responsible for 365 nm absorption. This absorption can lead to bulk phonons that contribute to desorption. Photon-induced desorption clearly plays an important role in the NO/MgO(100) system and may also be important in ClNO/MgO(100) at both low and high coverages. Desorption is generally driven by the substrate and the NO/MgO(100) experiment shows clearly that the MgO crystal can play a more active role in photon-induced processes—at least at low coverages—than is surmised from its inertness and 365 nm transparency.

The observed fragment cooling may also result from quenching in islands on the surface. Recent work by Huber and co-workers on methyl nitrate provides an example of such a phenomenon.[45] In that work, the NO vibrational and rotational state distributions resulting from the 364 nm photolysis of CH_3ONO monomers and clusters were compared. Vibrational distributions were identical for monomers and clusters, suggesting that initial excitation is same in both cases. However, some of the NO was rotationally very cold and had little translational energy. The cooling of NO in the ClNO/MgO(100) system may occur by a mechanism similar to that observed by Huber and co-workers in gas-phase methyl nitrate clusters. Our TPD data are consistent with the formation of islands in ClNO/MgO(100), and, if these are nucleated at point defects or steps at the surface, the persistence of photofragment cooling to very low coverages can be explained. The microscopic mechanism is still unknown, and the possibility that the surface is also involved, especially at low coverages, remains open; i.e., NO photolysis fragments, even from an isolated $ClNO_{(a)}$ molecule, may be cooled by interactions with the surface.

Loss of fragment rotational and translational energies in islands may also lead to some ClNO desorption, which may explain why the TOF data obtained with QMS1 are consistent with some desorption of intact ClNO, though REMPI detection does not reveal rotationally hot NO from photodissociation of desorbed ClNO. We note that in the photolysis of adsorbed methyl iodide, both gas-phase and surface dissociation products were identified clearly by REMPI indicating that photoexcitation leads to dissociation on the surface as well as desorption of methyl iodide, which is then photolyzed with the same laser pulse.[24,28,30] For ClNO, the gas-phase desorption cross section at 365 nm is 1.2×10^{-19} cm^2,[46] while the upper limit to the photodissociation cross section on MgO is 4.0×10^{-19} cm^2,[31] so photodissociation should be the primary outcome of 365 nm photoexcitation. However, since 1.8 eV is available to photoproducts, relaxation of hot fragments within ClNO islands should lead to local heating and possibly evaporation. If such desorption occurs after the photolyzing pulse, products from gas-phase ClNO photodissociation will not be detected.

Mechanisms related to the electronic structure of ClNO/MgO(100) should also be considered. Though a pure MgO crystal does not absorb near 365 nm, defect states within the band gap have been suggested.[37] No differences were observed in the TOF distributions for $\Theta=0.1$ and 0.02 L, and the TPD spectra indicate that these low coverages, isolated ClNO molecules are probably attached to defect sites whose electronic interactions with ClNO are unknown.

Little is known about the electronic structure of physisorbed ClNO in its ground and excited electronic states, nor

its geometry on the surface. Only recently have electronic structure calculations of adsorbates on MgO been reported.[43] McCarthy and Hess constrained Cl_2 to a perpendicular geometry and investigated its interactions with MgO(100) using the *ab initio* periodic Hartree–Fock LCAO method.[43] They found that Cl_2 binds to the oxygen with an energy of 4.1 kcal mol^{-1}, showing very little charge transfer between the surface and the molecule. An electrostatic potential based on quadrupole–dipole interactions could explain the binding qualitatively. The net molecule–surface interaction involved contributions from the $3s$ and $3p$ orbitals of Cl in Cl_2 and the $2s$ and $2p$ orbitals of oxygen in MgO.

The situation with ClNO adsorbed on MgO may be different. First, in the ground electronic state, the electrostatic interaction will be dominated by dipole–dipole forces, since *ab initio* calculations on free ClNO show significant negative charge on Cl and O and a positive charge on N.[34] It is possible then that ClNO will lie preferentially parallel to the surface, which is compatible with energy transfer to the surface. Second, the electronic interactions with the surface may be different in the ground and excited states, particularly in the parallel adsorption geometry. In the free molecule, the $S_3 \leftarrow S_0$ transition promotes a nonbinding Cl $3p$ electron which is perpendicular to the ClNO plane to a π^* orbital on NO, which is also perpendicular to the plane, resulting in a dipole moment oriented oppositely to the ground state.[34] On the surface, the half-filled $3p$ orbital on Cl and the π^* orbital on NO may interact with the surface prior to dissociation. Thus, the excited state electronic structure and the resulting forces and torques during dissociation may be quite different on the surface and in the gas phase.

The lack of strong dependence of the Cl^+ and NO^+ signals measured by QMS1 on the photolysis beam polarization may be a result of excitation of surface defect-induced electronic states, a bulk phonon desorption-based mechanism or specific adlayer structures. However, should it be the case that the signals observed at $m/e=35$ and 30 are due mostly to intact photodesorbed ClNO, the variation of intensity of dissociation products due to variation of the polarization might be difficult to detect even if the adlayer structure is such that polarization is important in the primary photolysis event. The polarization effect, if present, would be better observed with REMPI, which is sensitive only to the NO fragment. However reasonable REMPI measurements of NO fragments were only possible at above 0.7 L, and were also independent of the laser polarization.

V. SUMMARY

The photon-induced behavior of ClNO adsorbed at 90 K on MgO(100) that has been annealed in O_2 has been studied following 365 nm irradiation. Though oxygen vacancies have been largely eliminated, TPD data both on ClNO and NO indicate that a limited number of more strongly binding sites still exists; these saturate near 0.3 L. The results reported here with a smooth surface are similar to those obtained previously with a much rougher surface:[31] (i) products are translationally cold, with a broad TOF distribution; (ii) NO dissociation products interrogated by REMPI have similar TOF distributions to those obtained by monitoring NO^+ mass spectrometrically; (iii) NO rotational distributions show thermal equilibration with the cold surface; and (iv) no dependence on surface coverage or on laser polarization is observed.

Thus, even on inert insulating surfaces with adsorbate photolysis the primary event, large differences can exist between gas-phase and surface photochemistries. Intermolecular interactions that depend on adsorbate geometry as well as electronic effects can be important. For example, relaxation with ClNO islands or directly to the surface can cool fragments efficiently, and the transferred energy may also cause delayed desorption of ClNO. Effects such as light absorption by the crystal at defect sites followed by phonon production, or surface-induced changes in the electronic structure of excited ClNO, may also contribute to differences between gas-phase and surface photolyses. Some of the results can be rationalized more easily if ClNO is assumed to lie roughly parallel to the MgO(100) surface, as indicated by *ir* studies of ClNO thin films on CsI.[47] A direct determination of the geometry of ClNO on MgO(100), as well as electronic structure calculations, are needed before more definitive statements can be made.

ACKNOWLEDGMENTS

The authors thank E. Weitz for providing advice regarding the preparation of smooth MgO(100) crystals and B. E. Koel for valuable discussions. H.F. thanks the Deutsche Forschungsgemeinschaft for a fellowship. Research supported by the U.S. Air Force Office of Scientific Research.

[1] E. B. D. Bourdon. J. P. Cowin, I. Harrison, J. C. Polanyi, J. Segner, C. D. Stanners, and P. A. Young, J. Phys. Chem. **88**, 6100 (1984).
[2] E. B. D. Bourdon, P. Das, I. Harrison, J. C. Polanyi, J. Segner, C. D. Stanners, R. J. Williams, and P. A. Young, Faraday Discuss. Chem. Soc. **82**, 343 (1986).
[3] F. L. Tabares, E. P. Marsh, G. A. Bach, and J. P. Cowin, J. Chem. Phys. **86**, 738 (1987).
[4] T. J. Chuang and K. Domen, J. Vac. Sci. Technol. A **5**, 473 (1987).
[5] K. Domen and T. J. Chuang, Phys. Rev. Lett. **59**, 1484 (1987).
[6] St. J. Dixon-Warren, I. Harrison, K. Leggett, M. S. Matyjaszczyk, J. C. Polanyi, and P. A. Young, J. Chem. Phys. **88**, 4092 (1988).
[7] I. Harrison, J. C. Polanyi, and P. A. Young, J. Chem. Phys. **89**, 1475 (1988).
[8] I. Harrison, J. C. Polanyi, and P. A. Young, J. Chem. Phys. **89**, 1498 (1988).
[9] F. G. Celii, P. M. Whitmore, and K. C. Janda, J. Phys. Chem. **92**, 1604 (1988).
[10] C.-C. Cho, J. C. Polanyi, and C. D. Stanners, J. Chem. Phys. **90**, 598 (1988).
[11] J. Kutzner, G. Lindeke, K. H. Welge, and D. Feldmann, J. Chem. Phys. **90**, 548 (1989).
[12] K. Domen and T. J. Chuang, J. Chem. Phys. **90**, 3318 (1989).
[13] T. J. Chuang and K. Domen, J. Vac. Sci. Technol. B **7**, 1200 (1989).
[14] D. Feldmann, J. Kutzner, and K. H. Welge, in *Desorption Induced by Electronic Transitions DIET IV,* Springer Ser. Surf. Sci. Vol. 19, edited by G. Betz and P. Varga (Springer, Berlin, 1990).
[15] E. Villa, J. A. Dagata, and M. C. Lin, J. Chem. Phys. **92**, 1407 (1990).
[16] M. I. McCarthy, R. B. Gerber, and M. Shapiro, J. Chem. Phys. **92**, 7708 (1990).
[17] M. I. McCarthy and R. B. Gerber, J. Chem. Phys. **93**, 887 (1990).
[18] K. Leggett, J. C. Polanyi, and P. A. Young, J. Chem. Phys. **93**, 3645 (1990).
[19] St. J. Dixon-Warren, K. Leggett, M. S. Matyjaszczyk, J. C. Polanyi, and P. A. Young, J. Chem. Phys. **93**, 3659 (1990).
[20] J. C. Polanyi and P. A. Young, J. Chem. Phys. **93**, 3673 (1990).

[21] E. B. D. Bourdon, C.-C. Cho, P. Das, J. C. Polanyi, C. D. Stanners, and G.-Q. Xu, J. Chem. Phys. **95**, 1361 (1991).
[22] St. J. Dixon-Warren, M. S. Matyjaszczyk, J. C. Polanyi, H. Rieley, and J. G. Shapter, J. Phys. Chem. **95**, 1333 (1991).
[23] T. J. Chuang, R. Schwarzwald, and A. Mödl, J. Vac. Sci. Technol. A **9**, 1719 (1991).
[24] K. A. Trentelman, H. Fairbrother, P. C. Stair, P. G. Strupp, and E. Weitz, J. Vac. Sci. Technol. A **9**, 1820 (1991).
[25] T. J. Chuang, Lect. Notes Phys. **389**, 203 (1991).
[26] J. M. Watson, I. NoorBatcha, and R. R. Lucchese, J. Chem. Phys. **96**, 7771 (1992).
[27] (a) Z.-H. Huang and H. Guo, J. Chem. Phys. **96**, 8564 (1992); (b) **97**, 2110 (1992); (c) **98**, 3395 (1993).
[28] K. A. Trentelman, D. H. Fairbrother, P. G. Strupp, P. C. Stair, and E. Weitz, J. Chem. Phys. **96**, 9221 (1992).
[29] St. J. Dixon-Warren, R. C. Jackson, J. C. Polanyi, H. Rieley, J. G. Shapter, and H. Weiss, J. Phys. Chem. **96**, 10983 (1992).
[30] M. I. McCarthy, R. B. Gerber, K. A. Trentelman, P. Strupp, D. H. Fairbrother, P. C. Stair, and E. Weitz, J. Chem. Phys. **97**, 5168 (1992).
[31] L. Hodgson, G. Ziegler, H. Ferkel, H. Reisler, and C. Wittig, Can. J. Chem. (in press).
[32] G. N. A. Van Veen, T. Baller, and A. E. DeVries, Chem. Phys. **92**, 59 (1985).
[33] G. E. Busch and K. R. Wilson, J. Chem. Phys. **46**, 3655 (1972).
[34] (a) Y. Y. Bai, A. Ogai, C. X. W. Qian, L. Iwata, G. A. Segal, and H. Reisler, J. Chem. Phys. **90**, 3903 (1989); (b) A. Ogai, C. X. W. Qian, L. Iwata, and H. Reisler, Chem. Phys. Lett. **146**, 367 (1988).
[35] The terms "rough" and "smooth" are used in a qualitative sense. The MgO surface is referred to as smooth if it has been annealed in O_2 to remove oxygen vacancies. Otherwise, it is referred to as rough. See Sec. II for details.
[36] E. Kolodney, P. S. Powers, L. Hodgson, H. Reisler, and C. Wittig, J. Chem. Phys. **94**, 2330 (1991).
[37] V. E. Henrich and R. L. Kurtz, J. Vac. Sci. Technol. **18**, 416 (1981).
[38] (a) T. Kanaji, T. Kagotani, and S. Nagata, Thin Solid Films **32**, 217 (1976); (b) M. R. Welton-Cook and W. Berndt, J. Phys. C **15**, 5691 (1982); (c) T. Urano, T. Kanaji, and M. Kaburagi, Surf. Sci. **134**, 109 (1983); (d) A. Santoni, D. B. Tran-Thoai, and J. Urban, Solid State Commun. **68**, 1039 (1988).
[39] (a) G. Rowe and G. Ehrlich, J. Chem. Phys. **63**, 4648 (1975); (b) K. H. Riedler, Surf. Sci. **118**, 57 (1982); (c) G. Brusdeylins, R. B. Doak, J. G. Skofronick, and J. P. Toennies, *ibid.* **128**, 191 (1983); (d) P. Cantini and E. Cevasco, *ibid.* **148**, 37 (1984); (e) E. Kolodney and A. Amirav, *ibid.* **155**, 715 (1985); (f) C. Duriez, C. Chapon, C. R. Henry, and J. M. Rickard, *ibid.* **230**, 123 (1990).
[40] M. C. Bartelt and J. W. Evans, Phys. Rev. B **46**, 12675 (1992).
[41] For example: J. A. Venables, G. D. T. Spiller, and M. Hanbrücken, Rep. Prog. Phys. **47**, 399 (1984).
[42] J. P. D. Abbatt, D. W. Toohey, F. F. Fenter, P. S. Stevens, W. H. Brune, and J. G. Anderson, J. Phys. Chem. **93**, 1022 (1989).
[43] M. I. McCarthy and A. C. Hess, J. Chem. Phys. **96**, 6010 (1992).
[44] J. H. Crawford, Jr., in *Structure and Properties of MgO and Al_2O_3 Ceramics*, edited by W. D. Kingery (The American Ceramic Society, Columbus, OH, 1984).
[45] E. Kades, M. Rösslein, U. Brühlmann, and J. R. Huber, J. Chem. Phys. **97**, 989 (1993).
[46] C. Roehl, J. J. Orlando, and J. G. Calvert, J. Photochem. Photobiol. A: Chem. **69**, 1 (1992).
[47] L. H. Jones and B. I. Swanson, J. Phys. Chem. **95**, 86 (1991).